2-10-2020

# Probabilistic Hazard Assessment of Contaminated Sediment in Rivers

Shahab Aldin Shojaeezadeh
*Shiraz University*

Mohammad Reza Nikoo
*Shiraz University*

Ali Mirchi
*Oklahoma State University*

Iman Mallakpour
*University of California*

Amir AghaKouchak
*University of California*

*See next page for additional authors*

## Publication Information

Shojaeezadeh, Shahab Aldin; Nikoo, Mohammad Reza; Mirchi, Ali; Mallakpour, Iman; AghaKouchak, Amir; and Sadegh, Mojtaba. (2020). "Probabilistic Hazard Assessment of Contaminated Sediment in Rivers". *Science of The Total Environment, 703*, 134875-1 - 134875-15. https://doi.org/10.1016/j.scitotenv.2019.134875

This is an author-produced, peer-reviewed version of this article. The final, definitive version of this document can be found online at *Science of the Total Environment*, published by Elsevier. Copyright restrictions may apply. doi: 10.1016/j.scitotenv.2019.134875

# Probabilistic Hazard Assessment of Contaminated Sediment in Rivers

**Shahab Aldin Shojaeezadeh**
Department of Civil and Environmental Engineering
Shiraz University
Shiraz, Iran

**Mohammad Reza Nikoo**
Department of Civil and Environmental Engineering
Shiraz University
Shiraz, Iran

**Ali Mirchi**
Department of Biosystems and Agricultural Engineering
Oklahoma State University
Stillwater, OK, USA

**Iman Mallakpour**
Department of Civil and Environmental Engineering
University of California
Irvine, California, USA

**Amir AghaKouchak**
Department of Civil and Environmental Engineering
University of California
Irvine, California, USA

and

Department of Earth System Sciences
University of California
Irvine, California, USA

**Mojtaba Sadegh***
Department of Civil Engineering
Boise State University
Boise, ID, USA
mojtabasadegh@boisestate.edu

## Abstract

We propose a probabilistic framework rooted in multivariate and copula theory to assess heavy metal hazard associated with contaminated sediment in freshwater rivers that provide crucial ecosystem services such as municipal water source, eco-tourism, and agricultural irrigation. Exploiting the dependence structure between suspended sediment concentration (SSC) and different heavy metals, we estimate the hazard probability associated with each heavy metal at different SSC levels. We derive these relationships for warm (spring-summer) and cold (fall-winter) seasons, as well as stormflow condition, to unpack their nonlinear associations under different environmental conditions. To demonstrate its efficacy, we apply our proposed generic framework to Fountain Creek, CO, and show heavy metal concentration in warm season and under stormflow condition bears a higher hazard likelihood compared to the cold season. Under both warm season and stormflow conditions, probability of exceeding maximum allowable threshold for all studied heavy metals (Cu, Zn, and Pb, in recoverable form) at a standard hardness of 100 $mg/l\ CaCo_3$ and at a high level of SSC (95$^{th}$ percentile) is consistently more than 80% in our study site. Moreover, a longitudinal study along the Fountain Creek demonstrates that urban and agricultural land use considerably increase likelihoods of violating water quality standards compared to natural land cover. The novelty of this study lies in introducing a probabilistic hazard assessment framework that enables robust risk assessment with important policy implications about the likelihood of different heavy metals violating water quality standards under various SSC levels.

**Keywords:** contaminated sediment; heavy metals; probabilistic hazard assessment; copula; conditional marginal distribution

## Introduction

Sediment is a major physical and chemical pollutant in rivers, lakes, and estuaries (Newcombe and MacDonald, 1991). From a physical perspective, sediment disperses in the column of water and limits penetration of sunlight, which could lead to depleting dissolved oxygen by aquatic vegetation (Garcia, 2007). From a chemical viewpoint, sediment acts as a medium that can transport heavy metals, nutrients, and Polychlorinated Biphenyls (PCBs) (Ongley, 1996).

This is an author-produced, peer-reviewed version of this article. The final, definitive version of this document can be found online at *Science of the Total Environment*, published by Elsevier. Copyright restrictions may apply. doi: 10.1016/j.scitotenv.2019.134875

Sediments that carry various pollutants, referred to as contaminated sediments (Cui et al., 2008), have historically posed an important environmental management challenge in the US (Armitage, 2018). Remediation of contaminated sediments in various bodies of water in the US has imposed a cumulative cost of $33 billion since the Superfund Act in 1980 (Reible, 2014; Spellman, 2017).

Various indices, including degree of contamination (DC) (e.g. Abrahim and Parker, 2007), contamination factor (CF) (e.g. Varol, 2011), enrichment factor (EF) (Kumari et al., 2008), geoaccumulation index (Igeo) (Çevik et al., 2009; Ali et al., 2018) and sediment quality guideline-quotient (SQG-Q) (Caeiro et al., 2005) have been developed to assess and classify the degree of pollution due to contaminated sediments with reference to the corresponding guidelines and regulations. For example, Zhang et al. (2009) used geoaccumulation index and showed Cd, Cr and Ni enrichment in Yangtze River, China, is widespread, whereas Cu, Mn, Pb, and Zn are localized or non-existent. Geoaccumulation index is also used to determine the contamination level in the Tigris River, Turkey (Varol and Şen 2012), Korotoa River, Bangladesh (Saiful et al. 2015), Yellow River, China (Ma et al. 2016) and River Po, Hungary (Farkas et al. 2007), among others. Another example is Sakan et al. (2009) that used enrichment factor to evaluate various heavy metals pollution levels in Tisza River, Serbia. The authors also employed a modified Tessier method to analyze binding mechanisms of various heavy metals to sediments and thereby determined the source of pollutants. Other studies used a suite of different indices, including enrichment factor, contamination factor, pollution load index and geoaccumulation index, for assessment of heavy metal contamination in sediments (Varol, 2011).

Multivariate methods and clustering analysis are used to model the interrelation among pollutants and identify the driving variables of heavy metal pollution (Soares, 1999; Yongming et al., 2006; Chen et al., 2014). Yalchin et al. (2008), for example, used correlation and dendrogram hierarchical cluster analysis, and showed heavy metals that have high strong positive relations generally share the same source. A rather similar approach was adopted by Qu and Kelderman (2001) to determine the sources of pollution in Rhine River and Delft City canals in the Netherlands. This study gathers sediment samples along the Rhine river and from various canals, and uses factor analysis to analyze various characteristics of the studied pollutants. The authors showed Rhine River is an external source for micro-pollutants in the Delft City canals. Another example is the study of Liu et al. (2016) that used bivariate relationships between heavy metals and sediment to determine the anthropogenic and natural sources of heavy metals in Nanling, China. They first preprocessed observed data using centered log ratio and k-means clustering to minimize potentially spurious correlation among variables, and then employed factor analysis and compositional data analysis for this purpose.

Principal Component Analysis (PCA) is employed in the literature to detect the source of pollutants by reducing insignificant variables and follow the pollution information along the course of the river (Micó et al., 2006; Varol and Şen, 2012). For example, Wang et al. (2014) used a PCA analysis and showed that Zn, Pb, As, Hg, and Cd originate from industrial wastewater and domestic sewage, Cu, Co, and Fe are sourced from natural weathering and erosion, and Cr and Ni originate from agricultural and municipal areas along the Yangtze River China. Similarly, Passos et al. (2010) used PCA to cluster various heavy metals in Poxim river estuary, Brazil, and analyze the source location for each contaminant group. While majority of the contaminated sediment literature are focused on estuaries and lakes (Zoumis et al., 2001; Pignotti et al., 2018), hazard assessment of contaminated sediments and heavy metals in rivers has received increasing attention in the recent decade (Pejman et al., 2015; Wojtkowska et al, 2016; Patel et al., 2018; Pandey et al., 2019).

This paper presents a probabilistic framework for multivariate hazard assessment of contaminated sediment. This approach employs multivariate analysis with copulas to model the correlation structure between different heavy metal pollutants (in recoverable form) and suspended sediment concentration (SSC) to assess the probability of pollutant agents exceeding the EPA allowable thresholds at different SSC levels. We narrow down our analysis to warm and cold seasons, in addition to stormflow condition, in order to examine the interdependency between SSC and heavy metals under different ambient conditions. The seasonal analysis also allows us to investigate the effects of different parameters such as pH, temperature and specific conductance on SSC-heavy metal correlation structure. Finally, we evaluate the land use and land cover effects on the concentration of pollutants and SSC along example stream sections, showing that urban and agricultural land uses significantly increase heavy metal pollutant concentrations. Novelty of this study lies in the introduction of a robust probabilistic heavy metal hazard assessment framework with roots in multivariate and copula theory that provides significant risk-based insights to inform optimal management of contaminated sediments. Results can help ensure sustained ecosystem services, secure stakeholders' benefits, and avoid costly remediation efforts.

## Materials and Methods

### Probabilistic Hazard Assessment Framework

We first analyze the dependence between SSC and each pollutant using Pearson correlation coefficient. Note that other metrics such as mutual information (e.g. Khorshidi et al. 2018) or rank correlation coefficients can also be used for this purpose. When existence of statistically significant correlation (95% confidence level) between different variables is established (see Table S1, in Supplementary Information, SI), we model the marginal distributions of SSC and heavy metals using the 17 continuous distribution functions from Sadegh et al. (2018b). The best marginal distributions are selected according to Bayesian Information Criterion (BIC, Schwarz, 1978; Fig. 1 B1-B2). BIC is a statistical measure to select the best statistical model from a finite set of models:

$$\mathrm{BIC} = k\ln(n) - 2\ln(\hat{L}) \tag{1}$$

in which, $k$ represents model complexity (number of model parameters), $n$ signifies number of observations (length of data), and $\hat{L}$ symbolizes maximum likelihood. Likelihood indicates the probability that a set of observations belong to different sets of model parameters. Lower values of BIC associate with more desirable models. For more details about likelihood functions refer to Sadegh et al. (2017).

Marginal distributions are in turn used to construct copula models to represent the joint distribution of SSC and various pollutants. Copulas can explain the joint cumulative distribution of two (or more) time-independent random variables (Sklar's theorem; Sklar, 1959, Joe, 2015) regardless of their marginal distribution forms (De Michele et al., 2004; Nelsen, 2006):

$$H(x,y) = P(x \le X, y \le Y) = C(u_1,u_2), \qquad x,y \in R, \tag{2}$$

in which $H(x,y)$ is joint distribution, $u_1 = F(x) = P(x \le X)$ and $u_2 = G(y) = P(y \le Y)$ are marginal distributions of SSC and each heavy metal, respectively. Copula function, $C$, then maps $I \times I$ ($I \in [0,1]$) space to $I$. For example, Joe copula (Joe, 2005) is defined as:

$$C(u_1,u_2) = 1 - \left[(1-u_1)^\theta + (1-u_2)^\theta - (1-u_1)^\theta(1-u_2)^\theta\right]^{\frac{1}{\theta}}, \quad \theta \in [1,\infty), \tag{3}$$

in which, $\theta$ is a parameter to be tuned through an optimization algorithm (e.g. Naeini et al., 2018). We use the 25 built-in copula functions in the Multivariate Copula Analysis Toolbox (MvCAT; see Table 1 in Sadegh et al. (2017)), which is publicly available at http://amir.eng.uci.edu/MvCAT.php. The best copula model to describe the nonlinear dependence structure of SSC and each heavy metal is also selected based on BIC (Fig. 1C).

The dependence structure between SSC and heavy metals provides the basis for developing the probabilistic hazard assessment framework. This approach uses Bayesian networks and probability theory to derive the conditional marginal distribution of heavy metal depending on SSC using

$$f(u_2|u_1) = \frac{f(u_1,u_2)}{f(u_1)} \tag{4}$$

This is an author-produced, peer-reviewed version of this article. The final, definitive version of this document can be found online at *Science of the Total Environment*, published by Elsevier. Copyright restrictions may apply. doi: 10.1016/j.scitotenv.2019.134875

$f(u_2|u_1)$ represents conditional probability density function of variable $u_2$ depending on $u_1$, whereas $f(u_1, u_2)$ and $f(u_1)$ signifies joint probability density of $u_1$ and $u_2$, and marginal probability density function of $u_1$, respectively (Madadgar and Moradkhani, 2013). The joint probability density function is defined as (Shojaeezadeh et al., 2018):

$$f(u_1, u_2) = c(u_1, u_2)f(u_1)f(u_2) \tag{5}$$

in which, $c(u_1, u_2) = \frac{\partial^2 C(u_1,u_2)}{\partial u_1 \partial u_2}$ ($C$ representing copula joint cumulative distribution; Sadegh et al., 2018b). This transforms equation 4 to:

$$f(u_2|u_1) = \frac{f(u_1, u_2)}{f(u_1)} = \frac{c(u_1, u_2)f(u_1)f(u_2)}{f(u_1)} = c(u_1, u_2)f(u_2) \tag{6}$$

This conditional marginal distribution can then be used to estimate the likelihood of heavy metal concentrations ($u_2$) exceeding the EPA maximum allowable threshold given a certain level of SSC ($u_1$). In other words, this approach conditions the copula function on a specific level of SSC and multiplies the conditioned copula function (Fig. 1C, yellow surface) by the marginal distribution of the pollutant (Fig1. B2) to estimate the conditional marginal distribution of heavy metal given a certain level of SSC (Fig. 1D). The area under the curve of the conditional marginal distribution of the heavy metal above the maximum allowable threshold gives the likelihood of the hazard (red region in Fig. 1D).

## Hazard and Maximum Allowable Pollutant Level

We define hazard as heavy metal (or any pollutant) concentration exceeding maximum allowable threshold. We use the criterion maximum concentration (CMC) threshold, which is defined by EPA as maximum allowable level for point observation analysis. EPA also defines criterion continuous concentration (CCC) for chronic response to water pollution, which is not suited for this study due to the nature of available data (see Data section) (Santore et al., 2001; USEPA, 2007). The EPA maximum allowable thresholds for recoverable heavy metals are formulated based on the hardness of water (see Table S2 in SI).

## Data

We parameterize the proposed probabilistic model using suspended sediment concentration (SSC) and heavy metal concentration data obtained from the US Geological Survey (USGS) water quality portal (https://www.waterqualitydata.us/). Observations of SSC and heavy metal concentration are provided on a bi-weekly to monthly basis between 2000 to 2018 for active sites. The pollutant observations are classified into four categories: 1. Dissolved: solved in water, 2. Recoverable: adsorbed to sediment particles, 3. Suspended: in suspension form in the column of water, and 4. Total: sum of pollutants in all these categories. We set a threshold of availability of at least 35 concurrent observations of SSC and heavy metal concentration for selecting study sites to ensure capturing the variability of the system, and robustly parameterizing marginal and joint distributions (see Fig. S1 and refer to Ross (2009) for more details). We randomly select 77 USGS stations across the US that satisfy the selection criterion, and use Pearson correlation analysis to investigate the linear relationship between SSC and multiple heavy metal pollutants in dissolved, recoverable and total forms. The correlation structure between SSC and various heavy metals in these sites attest to the applicability of the proposed hazard assessment framework in different regions across the US and elsewhere. EPA regulates seven heavy metals, namely cadmium (Cd), chromium (Cr), copper (Cu), lead (Pb), nickel (Ni), silver (Ag) and zinc (Zn) in recoverable form (Armitage, 2018), which are analyzed herein. Table S1 presents the Pearson correlation coefficients between heavy metal concentration and SSC level for each studied station.

This is an author-produced, peer-reviewed version of this article. The final, definitive version of this document can be found online at *Science of the Total Environment*, published by Elsevier. Copyright restrictions may apply. doi: 10.1016/j.scitotenv.2019.134875

Heavy metal pollutants in recoverable form, expectedly, show positive correlation with SSC (displayed with light green), implying that increase in SSC level is associated with heightened pollutant level. Pearson correlation coefficients show that heavy metal concentrations in both recoverable and total forms have significantly higher positive correlations with SSC, as compared to the pollutants in the dissolved form. The close proximity of the Pearson correlation coefficients of pollutants in the total and recoverable forms with SSC implies that a great portion of the total pollutants is in the recoverable form. It is also interesting that dissolved lead and copper show statistically significant level of correlation with SSC, while interdependency for zinc in the dissolved form is weak across the 77 stations considered in this study. It is noteworthy that pollutant and SSC levels are observed at certain times (point measurement with bi-weekly to monthly frequency), and hence potential temporal lags between dissolved pollutants and SSC are not captured in the data we study herein. This might explain some of the negative correlation coefficients between dissolved pollutants and SSC. Desorption of pollutants from sediment and sorption into water, and vice versa, are influenced by flow conditions, pH and temperature, among others (Li et al., 2013). The temporal frequency of observations is not a cause for concern in a probabilistic modeling framework, i.e. static modeling, as long as the data constitute an adequate representation of the underlying marginal and joint distributions.

In this study, we investigate recoverable parameters to quantify the contaminated sediment hazard, since the nature of observed data (point observation) only warrants robust correlation structure between SSC and pollutants in recoverable form. Moreover, recoverable pollutants can be physically removed along with sediment at the source using Best Management Practices (BMPs) and various sediment trapping methods, which aligns with the purpose of the proposed methodology to provide risk-based information about contaminated sediment hazard to help decision-makers develop management plans. The methodology is generic and can also be effectively used for assessing hazards of dissolved heavy metals upon framing the correct underlying correlation structure.

## Case Study: Fountain Creek Watershed

We focus on the Fountain Creek at Colorado Springs, CO, as an example case and apply the proposed framework for probabilistic hazard assessment of contaminated sediments at USGS station 07105500. Particle size distribution (Fig. S2) shows that more than 60% of particles in this stretch of the river consists of silt and clay (grain size less than 0.0625 mm) with a high capacity for sorption of pollutants (Krishna and Mohan, 2013). Field observation of copper, lead, manganese, nickel and zinc concentrations as well as SSC are available for this station between 2000 and 2018, with a sampling gap between 2013 and 2015 (Fig. S3). Arsenic and mercury are two other major heavy metals, however, the data record does not provide enough observations for these pollutants in the recoverable form to be included in this analysis. Our investigation shows that Fountain Creek at Colorado Springs, CO, does not experience violation of water quality for manganese and nickel, and hence we merely focus on copper, zinc and lead in this paper. The proposed framework is generic and can be applied to all pollutant agents at any site.

We then extend our analysis to assess the impacts of land use and land cover on the hazard as this river flows from forest and barren land in its headwaters to downstream urban and agricultural lands. Multiple USGS stations along the Fountain Creek provide long-term observations of the required data enabling us to conduct this longitudinal analysis. We discuss the impacts of land use/cover on the SSC levels along this river, and investigate the hazards associated with different heavy metal violations.

Finally, we categorize the observed data into warm and cold seasons and stormflow condition to investigate the seasonal impacts and extreme event effects. Cold season consists of fall and winter, and warm season includes spring and summer. Stormflow condition is defined as streamflow exceeding 70$^{th}$ percentile of the observed flows (Shojaeezadeh et al., 2018).

# Results and Discussion

## Probabilistic Heavy Metal Hazard Assessment for Fountain Creek at Colorado Springs, CO

We first briefly discuss the impacts of various environmental parameters on the sorption and desorption of heavy metals to/from sediment particles, and present the statistics of each factor in the Fountain Creek at Colorado Springs, CO (USGS station 07105500). Fig. 2 presents observed ranges of zinc, copper, lead, discharge, pH, temperature, hardness and specific conductance for this station in warm and cold seasons as well as stormflow condition. pH values are consistently above 7 (alkali) with relatively small variation, with higher values in the cold season compared to the warm season, which is in turn greater than that of the stormflow condition. It is also noteworthy that variation of pH in the cold season is considerably lower than the warm season and stormflow condition. Several studies show that leachability of heavy metals from sediment particles is highly dependent on pH values (Eggleton and Thomas, 2004), however, weak acid and alkaline conditions, as observed in this station, leave minimal effects on sorption and desorption of heavy metals to/from sediment particles (Wang et al. 2016). Another effective parameter on pollutant sorption to sediment particle is temperature (Li et al., 2013). Temperature in this reach of the Fountain Creek varies widely between 0℃ to 25℃ throughout the year, which may bear contrasting effects on leachability of heavy metals from sediment particles (Echeverría et al., 2005).

Specific conductance and hardness are generally larger in the cold season compared to the warm season and stormflow condition. High value of specific conductance can facilitate desorption of pollution from sediment particles (Zhiming et al., 2013). Higher hardness values increase the maximum allowable thresholds for pollutant concentrations, i.e. promote higher tolerance for pollutants (Table S2). Fig. 2 also shows that concentrations of copper, zinc, and lead are higher for stormflow condition in comparison to warm season, which is in turn higher than that of the cold season. Variation of heavy metal concentrations is relatively small for stormflow condition and cold season, as opposed to the warm season that shows a large variability range. Finally, discharge values are higher for the stormflow condition, as expected, followed by warm and cold seasons, respectively. Higher discharges hold the required energy to transport suspended sediments, resuspend sediment particles from river bed, and wash river banks (Shajeezadeh et al., 2018).

We now evaluate the dependence level between SSC and various pollutants in the Fountain Creek at Colorado Springs, CO, which will be used to draw probabilistic inferences about the probability of hazard at different SSC levels. Fig. 3 shows Pearson correlation coefficients between SSC versus zinc, manganese, nickel, copper, lead, calcium, and magnesium concentrations in dissolved and recoverable form (based on the availability of observations) and other environmental factors such as discharge, hardness and specific conductance. While specific conductance, hardness and dissolved pollutants show a negative correlation with SSC, recoverable pollutants and streamflow portray positive correlation values with sediment (see Data section for a brief discussion on the causes). This is expected given that 60% of sediments in this reach of the Fountain Creek consist of small particles of clay and silt (Fig. S2) with high potential for sorption of heavy metals in recoverable form. Positive correlation between recoverable heavy metal concentrations and SSC implies higher levels of SSC bear higher potential for violating the maximum allowable limits for heavy metals, and hence posing a hazard.

We then use the proposed copula-based probabilistic framework to infer conditional marginal distribution of each heavy metal given various SSC levels ($5^{th}$, $10^{th}$, …, $95^{th}$ percentiles) to estimate the exceedance probability of the pollutant with reference to the EPA threshold. This involves fitting marginal and joint probability distributions, as described in the Methods section. Details of selected marginal and copula distributions for each case (based on BIC) are summarized in Table S3. Probability of copper, lead, and zinc concentrations exceeding EPA water quality standards are shown in Figs. 4-6, respectively. Each figure provides hazard assessment for one pollutant under cold season (A), warm season (B) and stormflow condition (C), which are referred to as environmental conditions, hereafter. For each environmental condition, we consider four hardness scenarios: (i) average, (ii) maximum, and (iii) minimum observed hardness levels, as well as (iv) hardness of 100 $mg/l\ CaCo_3$ (commonly used by EPA). We consider these four scenarios as maximum allowable threshold depends on water hardness (Table S2). Each figure lists all hardness values and associated maximum allowable thresholds for each heavy metal and each environmental condition. Each section of the figure includes several bins that represent the probability of pollutant concentrations exceeding the EPA threshold under $5^{th}$, $10^{th}$, $15^{th}$, …, $95^{th}$ percentiles of SSC levels. The SSC level associated with percentiles, obviously, differ between environmental conditions. Fig. S7 in SI presents the SSC values associated with different percentiles under each environmental condition for this reach of the Fountain Creek, CO.

Fig. 4 displays probabilities of hazard associated with copper under different environmental conditions and the four hardness scenarios. Copper in low concentration is an essential nutrient, but can be toxic to aquatic life in elevated concentrations (*Borkow and Gabbay, 2005). C*hronic exposure to copper can affect growth and reproduction of aquatic life and impair brain function, blood chemistry and metabolism in humans (Ahmad et al., 2010). Fig. 4A displays the probability of copper concentrations exceeding EPA thresholds in the cold season. Minimum (107 $mg/l\ CaCo_3$), average (243.1 $mg/l\ CaCo_3$), and maximum (354 $mg/l\ CaCo_3$) hardness levels in this station in the cold season are associated with maximum allowable recoverable copper thresholds of 14.92 $\mu g/l$, 32.33 $\mu g/l$, and 46.06 $\mu g/l$, respectively, whereas the copper threshold for hardness of 100 $mg/l\ CaCo_3$ is 13.99 $\mu g/l$. Only with extreme SSC level ($95^{th}$ percentile) and under minimum hardness (107 $mg/l\ CaCo_3$, most stringent threshold) is there a small probability (~20%) to violate the water quality standards. Thus, cold season will not pose a significant hazard

This is an author-produced, peer-reviewed version of this article. The final, definitive version of this document can be found online at *Science of the Total Environment*, published by Elsevier. Copyright restrictions may apply. doi: 10.1016/j.scitotenv.2019.134875

associated with copper for this river section. Under warm season and stormflow condition, however, the hazard has a much higher likelihood of occurrence. While the likelihood of recoverable copper posing a water quality hazard under low SSC levels ($5^{th}$-$15^{th}$ percentiles) for all hardness scenarios is minimal for the warm season (~0-5% likelihood), this increases to 40-90% likelihood under the stormflow condition (Figs. 4B-C) for a similar percentile range of SSC. Similarly, under medium range SSC levels ($45^{th}$-$55^{th}$ percentiles) the likelihood of violating the water quality standards is lower for the warm season (10-60%) in comparison to the stormflow condition (80-90%). However, the likelihood of such hazard under higher levels of SSC ($85^{th}$-$95^{th}$ percentiles) increases to 80-90% for both the warm season and streamflow conditions, except for the maximum hardness level (least stringent threshold for copper) in the warm season that is associated with a likelihood of 65%. See Fig. S7 in SI for the SSC levels associated with different percentiles under various environmental conditions.

Fig. 5 presents probabilistic hazard assessment of lead under different environmental conditions and various SSC levels. Lead is harmful to humans even under low concentrations, and can impair kidney function and induce hypertension, among several other long and short-term negative impacts (Jaishankar et al., 2014). Controlling lead is a high priority for EPA, especially after the high-profile incident of lead exposure through water distribution system between 2014-2015 in Flint, MI (Zahran et al., 2018). Lead, in the cold season in our study station, poses low risk of water quality violation, given lower levels of lead concentration in this season as well as higher hardness levels that promote less stringent thresholds (Fig. 5A). Indeed, for average hardness levels under different environmental conditions (243.1 $mg/l\ CaCo_3$, 162.1 $mg/l\ CaCo_3$ and 93.06 $mg/l\ CaCo_3$ for cold and warm seasons and stormflow condition, respectively), maximum allowable threshold for lead concentration is 252.9 μg/l in cold season, as compared to 151.0 $\mu g/l$ and 74.5 $\mu g/l$ for warm season and stormflow conditions. Lead hazard is more pronounced under stormflow condition as compared to warm season due to higher lead concentrations and more stringent maximum allowable thresholds. Under low SSC levels ($5^{th}$-$35^{th}$ percentile) in the warm season, likelihood of exceeding the lead maximum allowable threshold is between ~0% to ~7%, whereas this elevates to ~5% to ~60% for stormflow condition due to more stringent thresholds and higher lead concentrations (Fig. 5B-C). We can, however, compare the lead hazard under various environmental conditions with a common hardness of 100 $mg/l\ CaCo_3$, and hence a common maximum allowable threshold. In this case, cold season poses no hazard, even under high SSC levels, in terms of violating maximum allowable threshold for lead, but the likelihood of lead concentrations exceeding the threshold for warm season and stormflow condition exceeds 40% under median SSC levels ($45^{th}$ - $50^{th}$ percentile), and increases to 75-85% under higher SSC values ($85^{th}$-$95^{th}$ percentiles). Under minimum and constant (100 $mg/l\ CaCo_3$) hardness levels and for high SSC intensities, both warm season and stormflow conditions pose a very high likelihood of hazard (>80%).

We now move to hazard assessment for zinc in this reach of the Fountain Creek in Colorado. Zinc is an essential element for human and aquatic organisms' health in low concentrations (Santore et al., 2001; Naddy et al., 2015;). However, high concentrations of zinc can be very toxic and leave grave and sometimes irreversible effects on human health, such as stomach cramps, skin irritations and pancreas damage (Cooper et al., 2009; Fallah et al., 2018). Fig. 6 presents probabilistic assessment of zinc hazard under different environmental conditions. Similar to lead and copper, zinc does not pose a significant hazard in the cold season, while in the warm season and under stormflow condition, zinc hazard can be significant. Note, however, that lead and copper both show a gradual increase in the probability of exceeding maximum allowable threshold in response to rise in the SSC level in the warm season (Figs. 5B, 4B), whereas zinc hazard shows an abrupt rise when going from median (~$55^{th}$ percentile) to high (~$75^{th}$ to $95^{th}$ percentiles) SSC levels (Fig. 6B). For example, under average hardness level in the warm season (Fig. 6B), probability of zinc posing a hazard is nearly zero for the $65^{th}$ percentile SSC level, which escalates to ~60% for the SSC level of $75^{th}$ percentile. Similar behavior can be observed under different hardness scenarios in the warm season. There are two potential explanations for this behavior: (i) a small number of extreme events are driving the zinc violations. Therefore, associated SSC levels are culpable for exceeding the maximum allowable threshold (Fig S3), and (ii) the uncertainty in fitting marginal distributions and copulas can be translated into hazard assessment uncertainties (Sadegh et al., 2018a,b). Indeed, more extreme environmental conditions are associated with higher modeling uncertainties (Sadegh et al. 2018b). While uncertainty assessment is beyond the scope of this study, future users of the proposed methodology should be aware of the potential underlying uncertainties (see Sadegh et al. 2018a for example). Moreover, this framework bears an assumption of stationarity in the underlying processes, which can be violated by the impacts of watershed regulations and climate change (Sadegh et al., 2015; 2019). Our visual inspection as well as Mann-Kendall non-parametric trend analysis does not show any statistically significant trend in the data (Mallakpour et al. 2018; 2019).

This is an author-produced, peer-reviewed version of this article. The final, definitive version of this document can be found online at *Science of the Total Environment*, published by Elsevier. Copyright restrictions may apply. doi: 10.1016/j.scitotenv.2019.134875

## Impacts of Land Use and Land Cover on Heavy Metal Hazard in the Fountain Creek Watershed, CO

We conduct a longitudinal study along the Fountain Creek in Colorado to investigate the impacts of land use and land cover on the probability of hazard. Land use and land cover map of this watershed is shown in Fig. 7. Forest and woodland are dominant land cover in the upper reach of the river (middle fork) that mixes with semi desert and barren land before the first station of this analysis (A: USGS-07103700). Progressing downstream, majority of land cover evolves into developed and other urban human use (stations B: USGS-07103707, C: USGS-07105500, D: USGS-07105530). Further down the stream, agriculture becomes the dominant land use (E: USGS-07105800). Fig. 8 demonstrates SSC ranges obtained from the five USGS stations in this watershed under warm and cold seasons, as well as stormflow condition. From upstream to downstream, SSC levels increase, which is consistent with the impact of urban and agricultural land cover (Wang et al., 2007), with an exception of progressing from station A to B (Fig. 8). Comparing stations A and B, median SSC is generally higher for the downstream gauge, but the SSC range is generally wider for the upstream station; which could be attributed to the impact of deserted and barren land as well as the wildfires in the forests of the upstream of the river (Bartley et al., 2010; Miller and Stogner Robert, 2017). The SSC response follows a more consistent increasing trend as we proceed downstream from gauge B. Fig. 8 also shows the SSC range for warm season becomes more constrained from upstream to downstream, whereas this range increases for the cold season and stormflow conditions. Tighter ranges of SSC for the warm season is rather expected given limited precipitation events during summer with majority of the river flow being released from the upstream dams (Schwartz and Betancourt, 2013). The cold season and stormflow conditions, on the other hand, are associated with higher stochasticity in SSC concentrations as high intensity precipitation events in these periods introduce huge wash loads to the river (Shojaeezadeh et al., 2018).

We apply our probabilistic framework to quantify heavy metal hazard along the Fountain Creek, CO. For brevity, we present the hazard assessment results for copper in the warm season here, as Fountain Creek frequently observes copper violations in the warm season (also see Edelmann, 1990). Results for copper hazard assessment in the cold season and stormflow condition, as well as lead and zinc hazard assessment under various environmental conditions, are provided in the SI (Figs. S10 to S17). Fig. 9 shows hazard levels associated with copper for all five stations of the Fountain Creek in the warm season. As discussed previously, SSC levels increase from upstream to downstream, and given the positive association between SSC and heavy metals, pollution also increases along the river. This translates to generally higher probabilities of hazard, advancing from upstream to downstream (Fig. 9) due to additional copper contaminated sediment discharged into the river from urban and agricultural land. Hardness of water determines the maximum allowable threshold, and since hardness level changes between different stations, the associated threshold changes accordingly. These thresholds should be considered for cross comparison purposes. At a constant water hardness of 100 $mg/l\ CaCo_3$, we observe that for the upstream stations (Fig. 9A-B), the hazard is only likely for high SSC levels (associated with flood, Shojaeezadeh et al., 2018). As we move into the urban and agricultural land (Fig. 9C-E), however, the probability of hazard increases for both low and high SSC levels. For example, under $5^{th}$-$55^{th}$ percentile SSC levels for the upstream stations (A-B), the likelihood of copper concentrations exceeding the EPA threshold (at a hardness of 100 $mg/l\ CaCo_3$) is almost zero, which increases to about 5-60% in the downstream stations (C-E). This is in line with the findings in the literature that show a higher quantity of heavy metals are released from urban and agricultural areas to the river systems compared to that from the natural environment (Lubowski et al., 2016). Finally, this approach can pinpoint the pollution hot spots along the river using a risk-based approach. For example, stations C and D, corresponding to urban land use, bear a considerably higher hazard associated with lead (Fig. S12), compared to the upstream stations of A and B (natural land cover) and even the downstream station E (agricultural land use), for all SSC levels.

## Final Remarks

This analysis calls for proper sediment control and management for the warm season and stormflow condition, especially for high SSC levels. The hazard associated with heavy metal contaminated sediment is negligible in the cold season. The highest hazard level for copper, lead, and zinc in Fountain Creek at Colorado Springs, CO (USGS station 07105500) is expected under stormflow condition. Indeed, under stormflow condition, there is a high likelihood (~40-90%) of exceeding EPA maximum allowable threshold for copper and zinc, even at low SSC levels. This, however, is less extreme for lead, for which lower SSC levels are associated with significantly lower probabilities of water quality violations, i.e. ~0-20% (Fig. 5C). Lead poses a graver threat to human and animal health compared to copper and zinc (Jan et al. 2015). This hazard assessment approach should be used in the general risk framework, which takes into account exposure, vulnerability and hazard (Cardona et al. 2012). A 20% chance of violating water quality standard for lead, for example, might be associated with more treacherous consequences as compared to a 40% chance of violating the copper threshold. The proposed methodology enables probabilistic hazard assessment, making it useful for risk quantification by the decision-makers.

Finally, analysis of the impacts of land use and land cover shows that agricultural and urban land use are culpable for releasing high quantities of heavy metals to the Fountain Creek, substantially increasing the probability of hazard associated with heavy metal contaminated sediment. Our analysis of the hazard associated with copper, for example, shows that while probability of exceeding EPA thresholds for recoverable copper given lower than median SSC levels in the upper reaches of the Fountain Creek (forest and barren land cover) is negligible, it increases significantly as the river flows through urban and agricultural land cover. The proposed framework, hence, can also be used for longitudinal studies, and can inform risk-based feasibility and profitability assessments of potential Best Management Practices (BMPs).

## Conclusions

One major source of pollution in the rivers across the US is contaminated sediment. We propose a probabilistic framework rooted in multivariate theory that exploits the interrelation structure between sediment and heavy metals, and provides a robust assessment of contaminated sediment hazard. This approach models the marginal distribution of heavy metals and suspended sediment concentration (SSC), as well as joint distribution of the two variables using copulas. The copula function is then conditioned on a specific level of SSC, and multiplied by the marginal distribution of the pollutant, which returns conditional marginal distribution of the pollutant given the specified SSC level. The conditional marginal distribution of the pollutant is subsequently used to quantify the probability of pollutant concentration exceeding the EPA threshold level. Hazard is defined as violation of water quality standards, the likelihood of which is estimated by our proposed methodology.

We show in this paper that the proposed approach could be used to quantify the hazard level under different environmental conditions. It can also be used in longitudinal studies along the course of a river to identify pollution hot spots. This hazard assessment framework provides insights to where and when, and at what likelihood, potential hazards can occur. The probabilistic nature of this approach accommodates risk assessment studies, rendering it a valuable tool for watershed managers. Our results show there is a significant positive correlation between SSC and different heavy metals (including copper, lead and zinc) for multiple USGS stations. Hence, as SSC levels increase, hazard probability for different heavy metals elevates accordingly.

Our analysis also reveals that during warm season (spring and summer) and under stormflow condition, the probability of violating water quality standards is significantly higher than the cold season (fall and winter). For example, while the probability of violating maximum allowable threshold (under hardness of 100 $mg/l\ CaCo_3$) for recoverable copper in Fountain Creek, CO (USGS station 07105500) associated with high SSC level (95$^{th}$ percentile) is less than 20% for cold season, it increases to more than 90% under both warm season and stormflow condition. One explanation for this observation is that 95$^{th}$ SSC level in the summer season and stormflow condition is significantly higher than that of winter (Fig. S7), and hardness in winter is higher than that of the warm season and stormflow condition, which in turn relaxes the EPA standard thresholds. Similar observations are made for zinc and lead. Moreover, our longitudinal analysis shows that while the probability of exceeding maximum allowable threshold for recoverable copper in the upstream stations of the Fountain Creek in Colorado (forest and woodland land cover) given median SSC level (50$^{th}$ percentile) is negligible, it surges to above 80%-90% in the downstream stations as the river passes through agricultural and urban areas. Finally, our framework provides risk-based information to watershed managers as they prioritize their efforts to curb water quality violations.

## Abbreviations and Acronyms

| | |
|---|---|
| As | Arsenic |
| BIC | Bayesian Information Criterion |
| BMPs | Best Management Practices |
| Ca | Calcium |
| CaCo3 | Calcium Carbonate |
| CCC | Criterion Continuous Concentration |
| Cd | Cadmium |
| CF | Contamination Factor |
| CMC | Criterion Maximum Concentration |
| Co | Cobalt |
| Cr | Chromium |
| Cu | Copper |
| DC | Degree of Contamination |
| EF | Enrichment Factor |
| EPA | Environmental Pollution Agency |
| Fe | Iron |
| Hg | Mercury |
| Igeo | Geoaccumulation index |
| Mg | Magnesium |
| Mn | Manganese |
| Ni | Nickel |
| Pb | Lead |
| PCA | Principal Component Analysis |
| PCBs | Polychlorinated Biphenyls |
| SQG-Q | Sediment Quality Guideline-Quotient |
| SSC | Suspended Sediment Concentration |
| USGS | US Geological Survey |
| Zn | Zinc |

## Bibliography

Abrahim, G.M.S., Parker, R.J., 2008. Assessment of heavy metal enrichment factors and the degree of contamination in marine sediments from Tamaki Estuary, Auckland, New Zealand. Environmental Monitoring and Assessment 136, 227–238.

Ahmad, I., Ahamed, M., Pant, A.B., Akhtar, M.J., Siddiqui, M.A., Alhadlaq, H.A., 2010. Genotoxic potential of copper oxide nanoparticles in human lung epithelial cells. Biochemical and Biophysical Research Communications 396, 578–583.

Ali, A., Strezov, V., Davies, P.J., Wright, I., 2018. River sediment quality assessment using sediment quality indices for the Sydney basin, Australia affected by coal and coal seam gas mining. Science of The Total Environment 616–617, 695–702.

Armitage, T. M. (2018). EPA's contaminated sediment management strategy. In Metal Contaminated Aquatic Sediments (pp. 273-286). Routledge.

Atkinson, C.A., Jolley, D.F., Simpson, S.L., 2007. Effect of overlying water pH, dissolved oxygen, salinity and sediment disturbances on metal release and sequestration from metal contaminated marine sediments. Chemosphere 69, 1428–1437.

Bartley, R., Corfield, J.P., Abbott, B.N., Hawdon, A.A., Wilkinson, S.N., Nelson, B., 2010. Impacts of improved grazing land management on sediment yields, Part 1: Hillslope processes. Journal of Hydrology 389, 237–248.

Borkow, G., Gabbay, J., 2005. Copper as a Biocidal Tool. Current Medicinal Chemistry 12, 2163–2175.

Caeiro, S., Costa, M.H., Ramos, T.B., Fernandes, F., Silveira, N., Coimbra, A., Medeiros, G., Painho, M., 2005. Assessing heavy metal contamination in Sado Estuary sediment: An index analysis approach. Ecological Indicators 5, 151–169.

Cardona, O. D., van Aalst, M. K., Birkmann, J., Fordham, M., McGregor, G., & Mechler, R. (2012). Determinants of risk: exposure and vulnerability.

Çevik, F., Göksu, M.Z.L., Derici, O.B., Findik, Ö., 2009. An assessment of metal pollution in surface sediments of Seyhan dam by using enrichment factor, geoaccumulation index and statistical analyses. Environmental Monitoring and Assessment 152, 309–317.

Chen, H., Lu, X., Li, L.Y., Gao, T., Chang, Y., 2014. Metal contamination in campus dust of Xi'an, China: A study based on multivariate statistics and spatial distribution. Science of The Total Environment 484, 27–35.

Cooper, N.L., Bidwell, J.R., Kumar, A., 2009. Toxicity of copper, lead, and zinc mixtures to Ceriodaphnia dubia and Daphnia carinata. Ecotoxicology and Environmental Safety 72, 1523–1528.

Cui, X., Qiu, G., Peng, J., Yuan, P., Song, Y., 2008. The remediation of heavy metals contaminated sediment. Journal of Hazardous Materials 161, 633–640.

De Michele, C., Rosso, R., Petaccia, A., Canossi, M., Salvadori, G., 2004. Bivariate Statistical Approach to Check Adequacy of Dam Spillway. Journal of Hydrologic Engineering 10, 50–57.

Echeverría, J.C., Zarranz, I., Estella, J., Garrido, J.J., 2005. Simultaneous effect of pH, temperature, ionic strength, and initial concentration on the retention of lead on illite. Applied Clay Science 30, 103–115.

Edelmann, P., 1990. Water quality of Fountain and Monument creeks, south-central Colorado, with emphasis on relation of water quality to stream classifications, Water-Resources Investigations Report. U.S. Geological Survey.

Eggleton, J., Thomas, K.V., 2004. A review of factors affecting the release and bioavailability of contaminants during sediment disturbance events. Environment International 30, 973–980.

Fallah, A., Mohammad-Hasani, A., Colagar, A.H., 2018. Zinc is an essential element for male fertility: A review of zn roles in men's health, germination, sperm quality, and fertilization. Journal of Reproduction and Infertility 19, 69–81.

Farkas, A., Erratico, C., Viganò, L., 2007. Assessment of the environmental significance of heavy metal pollution in surficial sediments of the River Po. Chemosphere 68, 761–768.

Frank R Spellman, 2017. Contaminated Sediments in Freshwater Systems - Frank R. Spellman - Google Books. CRC Press, Taylor & Francis Group.

Garcia, M.H.C.N.-P. 1.-6480, 2008. Sedimentation engineering: processes, management, modeling, and practice.

Jan, A., Azam, M., Siddiqui, K., Ali, A., Choi, I., & Haq, Q. (2015). Heavy metals and human health: mechanistic insight into toxicity and counter defense system of antioxidants. *International journal of molecular sciences*, *16*(12), 29592-29630.

Joe, H. (2015). Dependence modeling with copulas. CRC Press, Taylor & Francis Group.

Joe, H., 2005. Asymptotic efficiency of the two-stage estimation method for copula-based models. Journal of Multivariate Analysis 94, 401–419.

Kelderman, P., Osman, A.A., 2007. Effect of redox potential on heavy metal binding forms in polluted canal sediments in Delft (The Netherlands). Water Res. 41, 4251–4261.

Khorshidi, M.S., Nikoo, M.R., Sadegh, M., 2018. Optimal and objective placement of sensors in water distribution systems using information theory. Water Research 143, 218–228.

Krishna, A.K., Mohan, K.R., 2013. Metal contamination and their distribution in different grain size fractions of sediments in an industrial development area. Bulletin of Environmental Contamination and Toxicology 90, 170–175.

Kumari, S., Kaushik, C.P., Kansal, A., Kaushik, A., Meena, Santosh, 2008. Heavy metal contamination of river Yamuna, Haryana, India: Assessment by Metal Enrichment Factor of the Sediments. Elsevier B.V.

Li, H., Shi, A., Li, M., Zhang, X., 2013. Effect of pH, Temperature, Dissolved Oxygen, and Flow Rate of Overlying Water on Heavy Metals Release from Storm Sewer Sediments. Journal of Chemistry 2013, 1–11.

Liu, Y., Cheng, Q., Zhou, K., Xia, Q., Wang, X., 2016. Multivariate analysis for geochemical process identification using stream sediment geochemical data: A perspective from compositional data. Geochem. J. 50, 293–314.

Lubowski, R.N., Bucholtz, S., Claassen, R., Roberts, M.J., Cooper, J.C., Gueorguieva, A., Lubowski, R.N., Bucholtz, S., Roberts, M.J., Cooper, J.C., Gueorguieva, A., Johansson, R., 2016. Environmental Effects of Agricultural Land-Use The Role of Economics and Policy The Role of Economics and Policy. USDA, Economic Research Service.

Ma, X., Zuo, H., Tian, M., Zhang, L., Meng, J., Zhou, X., Min, N., Chang, X., Liu, Y., 2016. Assessment of heavy metals contamination in sediments from three adjacent regions of the Yellow River using metal chemical fractions and multivariate analysis techniques. Chemosphere 144, 264–272.

Madadgar, S., Moradkhani, H., 2013. A Bayesian Framework for Probabilistic Seasonal Drought Forecasting. Journal of Hydrometeorology 14, 1685–1705.

Mallakpour, I., AghaKouchak, A., & Sadegh, M. (2019). Climate-induced changes in the risk of hydrological failure of major dams in California. Geophysical Research Letters, 46, 2130– 2139.

Mallakpour, I., Sadegh, M., & AghaKouchak, A. (2018). A new normal for streamflow in California in a warming climate: Wetter wet seasons and drier dry seasons. Journal of hydrology, 567, 203-211.

Micó, C., Recatalá, L., Peris, M., Sánchez, J., 2006. Assessing heavy metal sources in agricultural soils of an European Mediterranean area by multivariate analysis. Chemosphere 65, 863–872.

Miller, L.D., Stogner Robert W., S., 2017. Characterization of water quality and suspended sediment during cold-season flows, warm-season flows, and stormflows in the Fountain and Monument Creek watersheds, Colorado, 2007–2015, Scientific Investigations Report. Reston, VA.

Monisha, J., Tenzin, T., Naresh, A., B, M.B., N, B.K., 2014. Toxicity, mechanism and health effects of some heavy metals. Interdisciplinary Toxicology 7, 60.

Naddy, R.B., Cohen, A.S., Stubblefield, W.A., 2015. The interactive toxicity of cadmium, copper, and zinc to Ceriodaphnia dubia and rainbow trout (Oncorhynchus mykiss). Environmental Toxicology and Chemistry 34, 809–815.

Nelsen, R. B. (2006). An Introduction to Copulas. Springer Science Business Media.

Newcombe, C.P., Macdonald, D.D., 2004. Effects of Suspended Sediments on Aquatic Ecosystems. North American Journal of Fisheries Management 11, 72–82.

Ongley, E.D., n.d. Control of water pollution from agriculture. Published by arrangement with the Food and Agriculture Organization of the United Nationa by Daya Publ. House.

Pandey, L.K., Park, J., Son, D.H., Kim, W., Islam, M.S., Choi, S., Lee, H., Han, T., 2019. Assessment of metal contamination in water and sediments from major rivers in South Korea from 2008 to 2015. Science of The Total Environment 651, 323–333.

Passos, E. de A., Alves, J.C., dos Santos, I.S., Alves, J. do P.H., Garcia, C.A.B., Spinola Costa, A.C., 2010. Assessment of trace metals contamination in estuarine sediments using a sequential extraction technique and principal component analysis. Microchem. J. 96, 50–57.

Passos, E. de A., Alves, J.C., dos Santos, I.S., Alves, J. do P.H., Garcia, C.A.B., Spinola Costa, A.C., 2010. Assessment of trace metals contamination in estuarine sediments using a sequential extraction technique and principal component analysis. Microchemical Journal 96, 50–57.

Patel, P., Raju, N.J., Reddy, B.C.S.R., Suresh, U., Sankar, D.B., Reddy, T.V.K., 2018. Heavy metal contamination in river water and sediments of the Swarnamukhi River Basin, India: risk assessment and environmental implications. Environmental Geochemistry and Health 40, 609–623.

Pejman, A., Bidhendi, G., Ardestani, M., \ldots, M.S.-E., undefined 2015, n.d. A new index for assessing heavy metal contamination in sediments. Elsevier.

Pignotti, E., Guerra, R., Covelli, S., Fabbri, E., Dinelli, E., 2018. Sediment quality assessment in a coastal lagoon (Ravenna, NE Italy) based on SEM-AVS and sequential extraction procedure. Science of The Total Environment 635, 216–227.

Rahnamay Naeini, M., Yang, T., Sadegh, M., AghaKouchak, A., lin Hsu, K., Sorooshian, S., Duan, Q., Lei, X., 2018. Shuffled Complex-Self Adaptive Hybrid EvoLution (SC-SAHEL) optimization framework. Environmental Modelling and Software 104, 215–235.

Reible, D. D. (Ed.). (2014). Processes, assessment and remediation of contaminated sediments (pp. 365-391). New York: Springer.

Ross, S. M. (2009). Distributions of sampling statistics. In Introduction to Probability and Statistics for Engineers and Scientists (pp. 203-229). Academic.

Sadegh, M., AghaKouchak, A., Flores, A., Mallakpour, I., & Nikoo, M. R. (2019). A Multi-Model Nonstationary Rainfall-Runoff Modeling Framework: Analysis and Toolbox. Water Resources Management, 33(9), 3011-3024.

Sadegh, M., Moftakhari, H., Gupta, H.V., Ragno, E., Mazdiyasni, O., Sanders, B., Matthew, R., AghaKouchak, A., 2018a. Multihazard Scenarios for Analysis of Compound Extreme Events. Geophysical Research Letters 45, 5470–5480.

Sadegh, M., Ragno, E., & AghaKouchak, A. (2017). Multivariate Copula Analysis Toolbox (MvCAT): Describing dependence and underlying uncertainty using a Bayesian framework. Water Resources Research, 53(6), 5166-5183.

This is an author-produced, peer-reviewed version of this article. The final, definitive version of this document can be found online at *Science of the Total Environment*, published by Elsevier. Copyright restrictions may apply. doi: 10.1016/j.scitotenv.2019.134875

Sadegh, M., Shakeri Majd, M., Hernandez, J., Haghighi, A.T., 2018b. The Quest for Hydrological Signatures: Effects of Data Transformation on Bayesian Inference of Watershed Models. Water Resources Management 32, 1867–1881.

Sadegh, M., Vrugt, J.A., Xu, C., Volpi, E., 2015. The stationarity paradigm revisited: Hypothesis testing using diagnostics, summary metrics, and DREAM(ABC). Water Resources Research 51, 9207–9231.

Saiful, I., Kawser, A., Mohammad, R., Habibullah, A., Muhammad, K., 2015. Heavy metal pollution in surface water and sediment: A preliminary assessment of an urban river in a developing country. Ecol. Indic. 48, 282–291.

Sakan, S.M., Dordević, D.S., Manojlović, D.D., Predrag, P.S., 2009. Assessment of heavy metal pollutants accumulation in the Tisza river sediments. J. Environ. Manage. 90, 3382–3390.

Santore, R.C., Di Toro, D.M., Paquin, P.R., Allen, H.E., Meyer, J.S., 2001. Biotic ligand model of the acute toxicity of metals. 2. Application to acute copper toxicity in freshwater fish and Daphnia. Environmental Toxicology and Chemistry 20, 2397–2402.

Schwartz, M.D., Ault, T.R., Betancourt, J.L., 2013. Spring onset variations and trends in the continental United States: Past and regional assessment using temperature-based indices. International Journal of Climatology 33, 2917–2922.

Schwarz, G., 1978. Estimating the Dimension of a Model. Ann. Stat. 6, 461–464.

Shojaeezadeh, S.A., Nikoo, M.R., McNamara, J.P., AghaKouchak, A., Sadegh, M., 2018. Stochastic modeling of suspended sediment load in alluvial rivers. Advances in Water Resources 119, 188–196.

Sklar, A., 1959. Fonctions de répartition à n dimensions et leurs marges. Publications Inst. Statis., Univ. Paris-VIII 8, 229–231.

Soares, H.M.V.M., Boaventura, R.A.R., Machado, A.A.S.C., Esteves Da Silva, J.C.G., 1999. Sediments as monitors of heavy metal contamination in the Ave river basin (Portugal): Multivariate analysis of data. Environmental Pollution 105, 311–323.

USEPA National Recommended Water Quality Criteria for Freshwater and Human Consumption of Water + Organism: 2002, 2007, in: The Environmental Science of Drinking Water. Water, pp. 237–239.

Varol, M., 2011. Assessment of heavy metal contamination in sediments of the Tigris River (Turkey) using pollution indices and multivariate statistical techniques. J. Hazard. Mater. 195, 355–364.

Varol, M., 2011. Assessment of heavy metal contamination in sediments of the Tigris River (Turkey) using pollution indices and multivariate statistical techniques. Journal of Hazardous Materials 195, 355–364.

Varol, M., Şen, B., 2012. Assessment of nutrient and heavy metal contamination in surface water and sediments of the upper Tigris River, Turkey. Catena 92, 1–10.

Varol, M., Şen, B., 2012. Assessment of nutrient and heavy metal contamination in surface water and sediments of the upper Tigris River, Turkey. Catena 92, 1–10.

Wang, G., Shi, Y., Wang, T., Luo, W., Lu, Y., Giesy, J.P., Xing, Y., 2007. Effects of land use on concentrations of metals in surface soils and ecological risk around Guanting Reservoir, China. Environmental Geochemistry and Health 29, 459–471.

Wang, L., Wang, Y., Zhang, W., Xu, C., An, Z., 2014. Multivariate statistical techniques for evaluating and identifying the environmental significance of heavy metal contamination in sediments of the Yangtze River, China. Environ. Earth Sci. 71, 1183–1193.

Wang, P., Xue, Q., Li, J.S., Zhang, T.T., 2016. Effects of pH on leaching behavior of compacted cement solidified/stabilized lead contaminated soil. Environmental Progress and Sustainable Energy 35, 149–155.

Weiner, E., 2000. National Recommended Water Quality Criteria, in: Applications of Environmental Chemistry. CRC Press.

Wojtkowska, M., Bogacki, J., Witeska, A., 2016. Assessment of the hazard posed by metal forms in water and sediments. Science of The Total Environment 551–552, 387–392.

Yalcin, M.G., Narin, I., Soylak, M., 2008. Multivariate analysis of heavy metal contents of sediments from Gumusler creek, Nigde, Turkey. Environ. Geol. 54, 1155–1163.

Yongming, H., Peixuan, D., Junji, C., Posmentier, E.S., 2006. Multivariate analysis of heavy metal contamination in urban dusts of Xi'an, Central China. Science of the Total Environment 355, 176–186.

Zhang, W., Feng, H., Chang, J., Qu, J., Xie, H., Yu, L., 2009. Heavy metal contamination in surface sediments of Yangtze River intertidal zone: An assessment from different indexes. Environ. Pollut. 157, 1533–1543.

Zhiming, Z., Zhanbin, H., Ke, T., & Entong, L. (2013, August). The leaching research of environmental materials on Pb and Cd contaminated soil. Atlantis Press.

Zoumis, T., Schmidt, A., Grigorova, L., Calmano, W., 2001. Contaminants in sediments: remobilisation and demobilisation. Science of The Total Environment 266, 195–202.

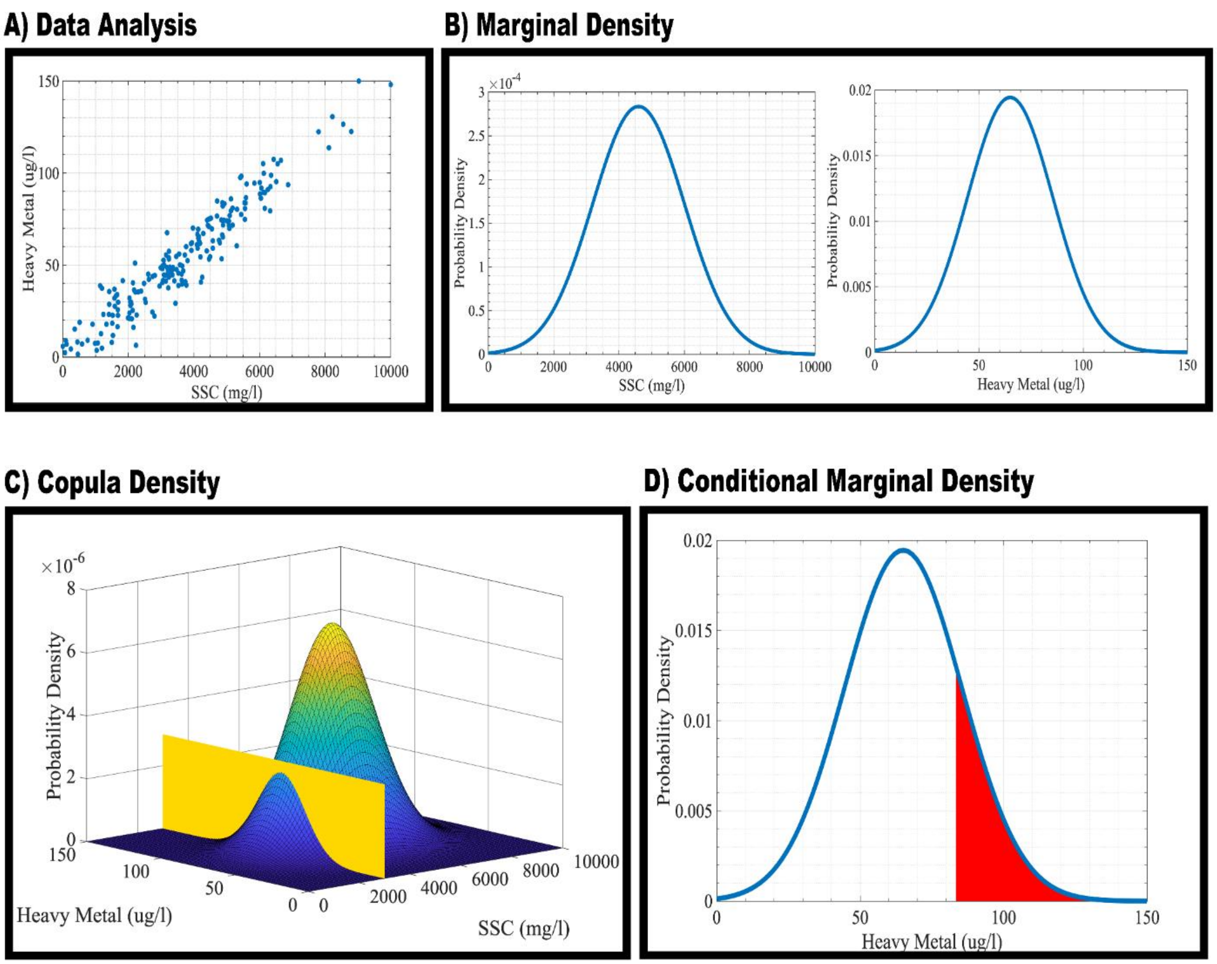


*Figure 1. Probabilistic hazard assessment framework for contaminated sediment: A: scatterplot of SSC and heavy metal observations, B1-2: marginal distributions of SSC and heavy metal, respectively, C: joint distribution of SSC and heavy metal, with yellow surface conditioning the joint distribution on a certain SSC level, D: conditional marginal distribution of heavy metal at a certain SSC level. Red area in plot D shows the probability of heavy metal concentrations exceeding a certain threshold.*

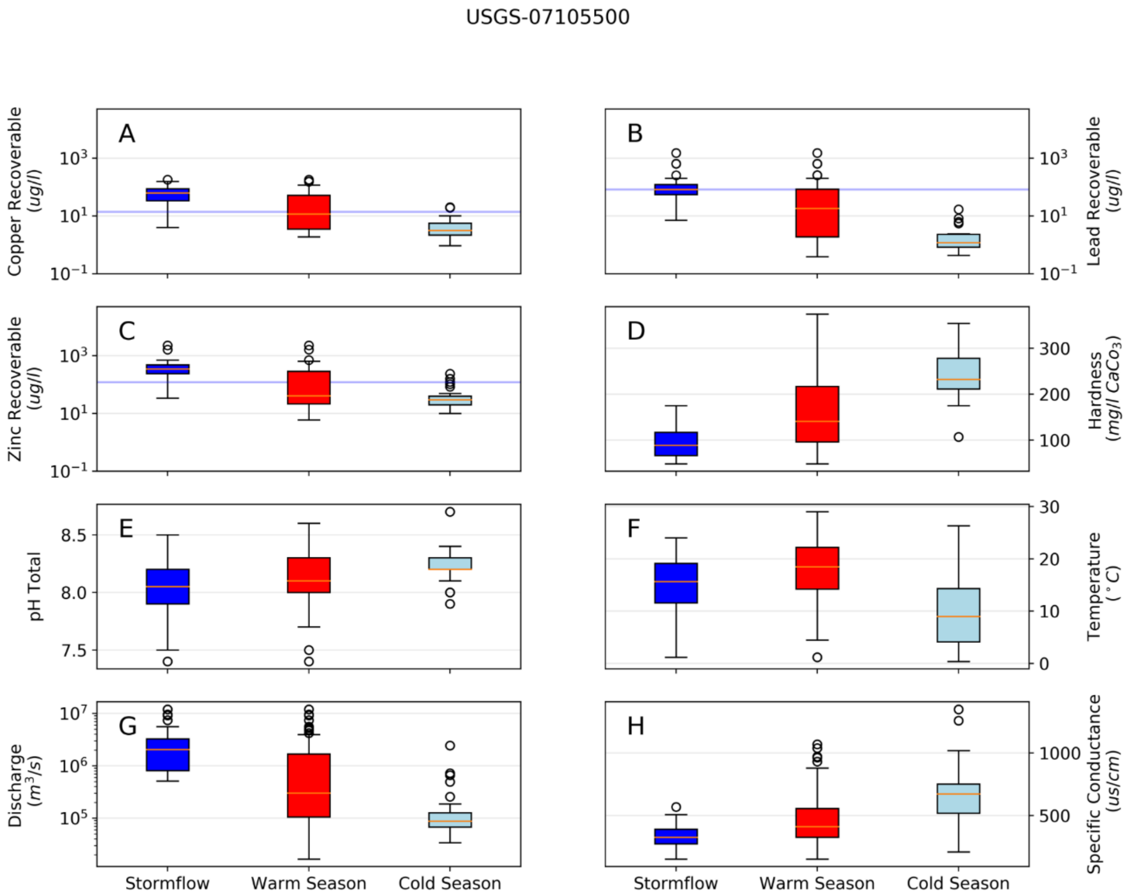


*Figure 2. Range of heavy metals and various ambient river parameters for Fountain Creek at Colorado Springs, CO (USGS-07105500) under warm (spring-summer) and cold (fall-winter) seasons and stormflow condition. Blue line is the EPA threshold for hardness equal to 100 $mg/l$ $CaCo_3$.*

This is an author-produced, peer-reviewed version of this article. The final, definitive version of this document can be found online at *Science of the Total Environment*, published by Elsevier. Copyright restrictions may apply. doi: 10.1016/j.scitotenv.2019.134875

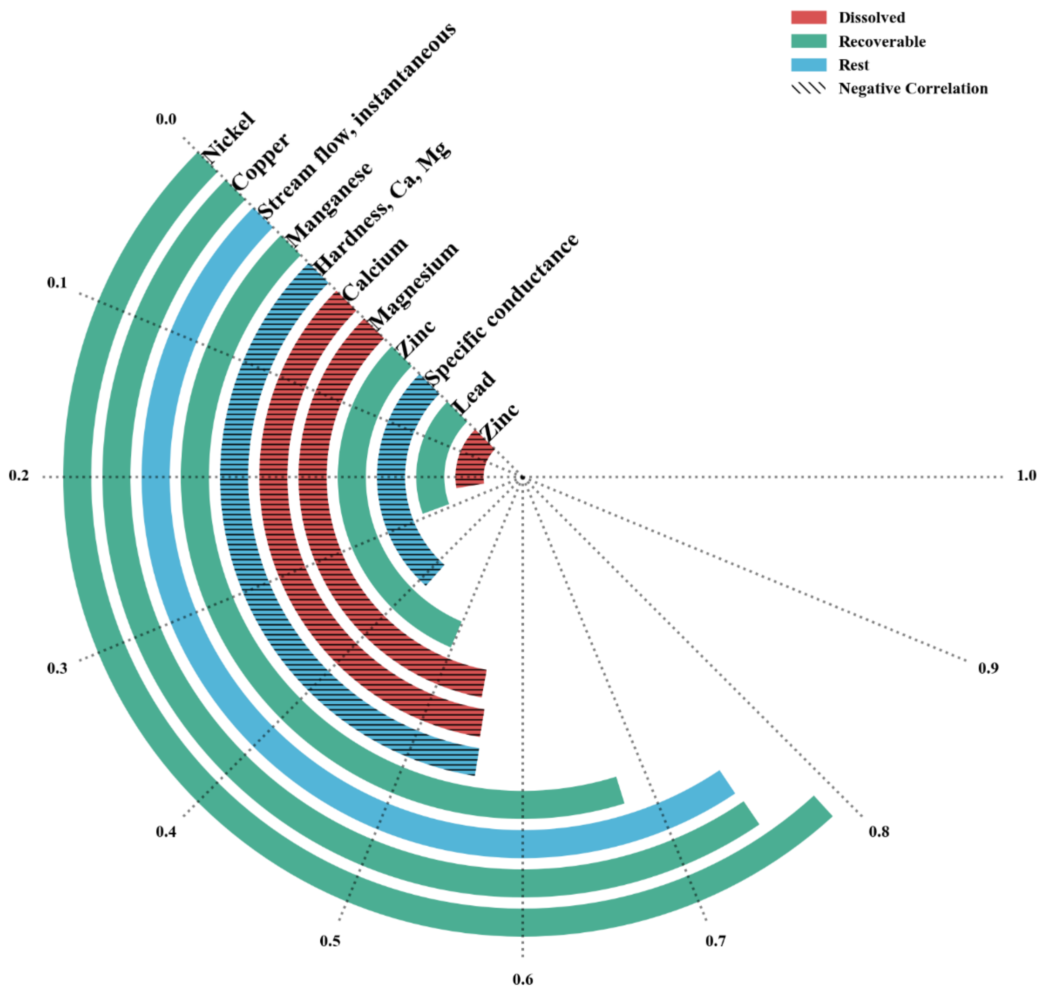


*Figure 3. Pearson correlation coefficient between suspended sediment concentrations and different heavy metal concentrations, as well as other ambient variables for Fountain Creek in Colorado (USGS station 07105500). Length of each radial bar shows the Pearson correlation coefficient value (between 0-1). Correlation is statistically significant at the 5% level.*

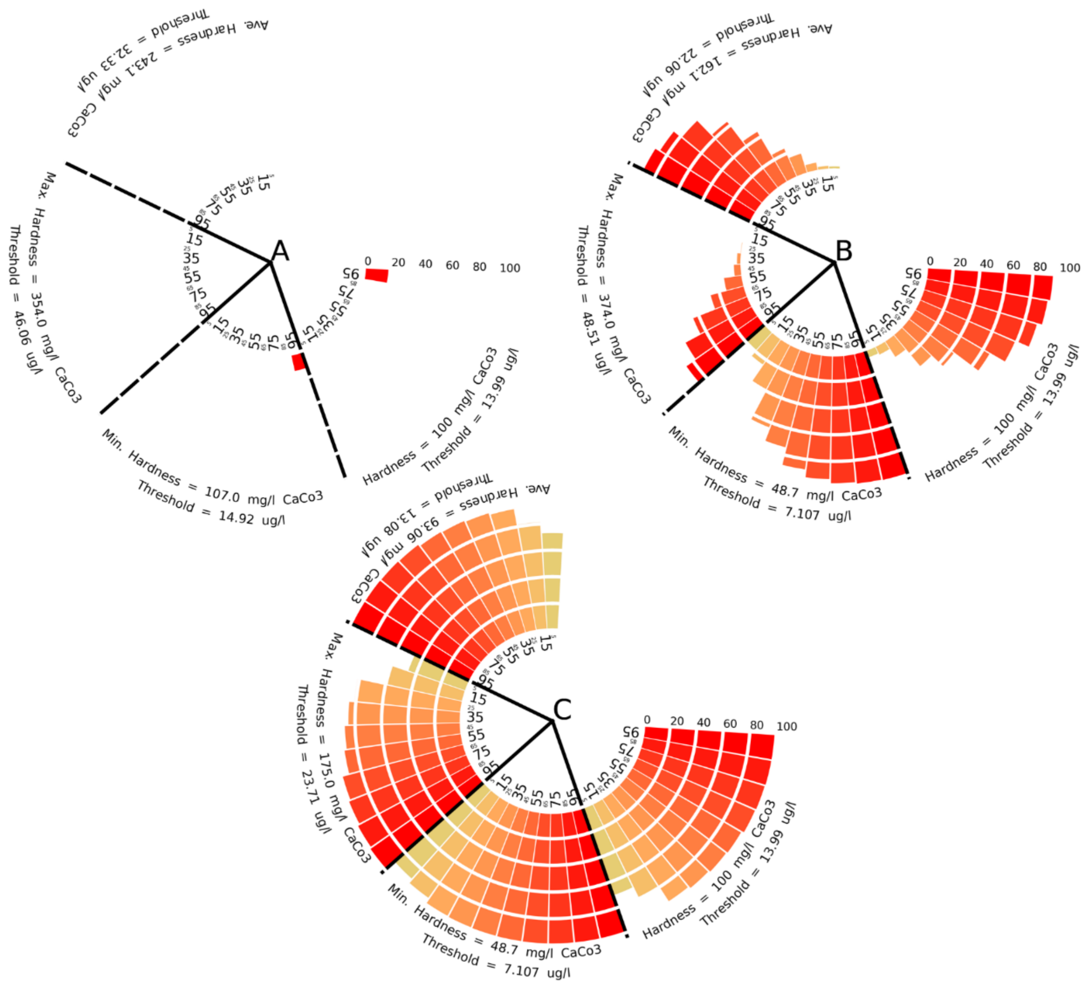


*Figure 4. Likelihood of hazard posed by copper concentration exceeding EPA maximum allowable threshold under different suspended sediment concentrations in cold season (A), warm season (B), and stormflow condition (C). Each plot includes four scenarios: average, minimum, and maximum observed hardness, as well as a constant hardness level of 100 $mg/l\ CaCo_3$, and their associated maximum allowable pollutant level. Each bin in each scenario is associated with one SSC level (percentile), the length of which represents probability of hazard. Bins are color-coded from yellow (low SSC level) to red (high SSC level).*

This is an author-produced, peer-reviewed version of this article. The final, definitive version of this document can be found online at *Science of the Total Environment*, published by Elsevier. Copyright restrictions may apply. doi: 10.1016/j.scitotenv.2019.134875

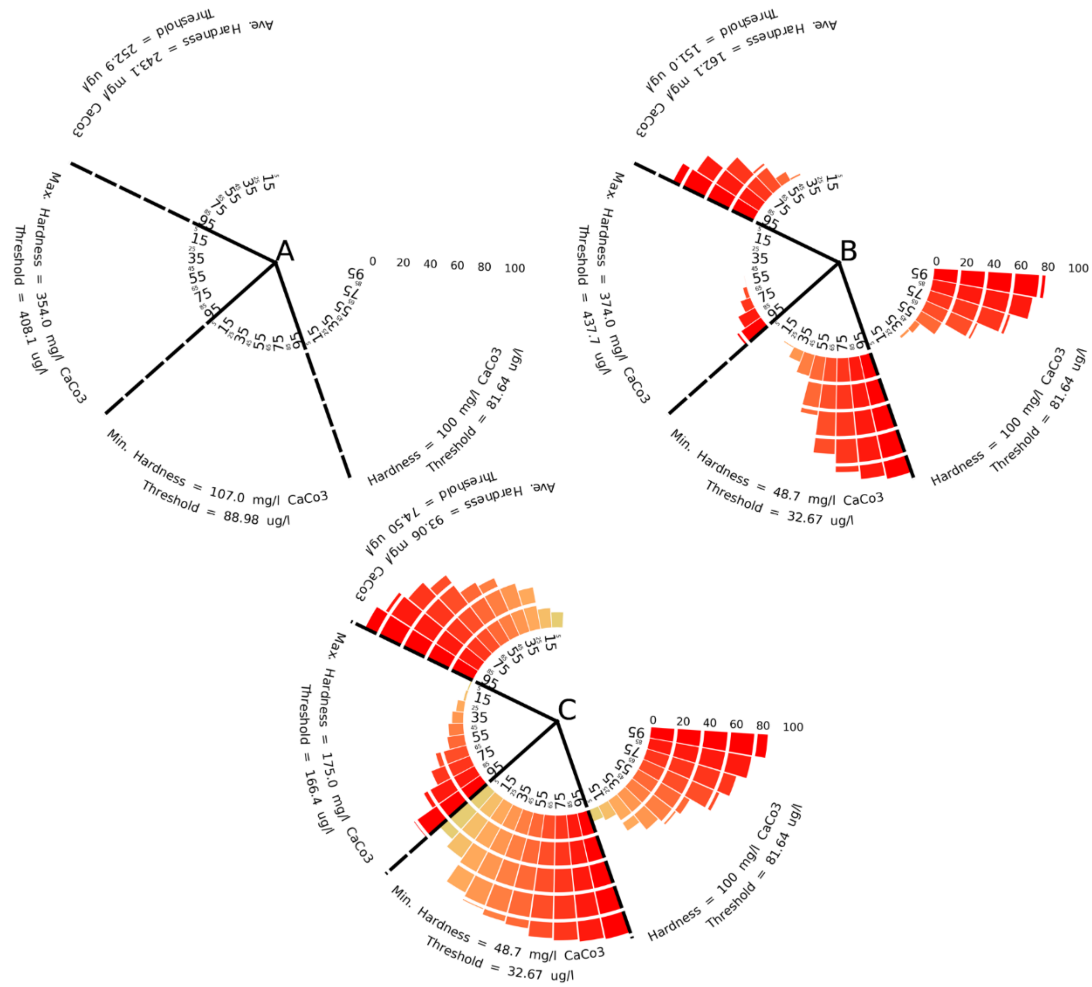


*Figure 5. Likelihood of hazard posed by lead concentration exceeding EPA maximum allowable threshold under different suspended sediment concentrations in cold season (A), warm season (B), and stormflow condition (C). Each plot includes four scenarios: average, minimum, and maximum observed hardness, as well as a constant hardness level of 100 /l $CaCo_3$, and their associated maximum allowable pollutant level. Each bin in each scenario is associated with one SSC level (percentile), the length of which represents probability of hazard. Bins are color-coded from yellow (low SSC level) to red (high SSC level).*

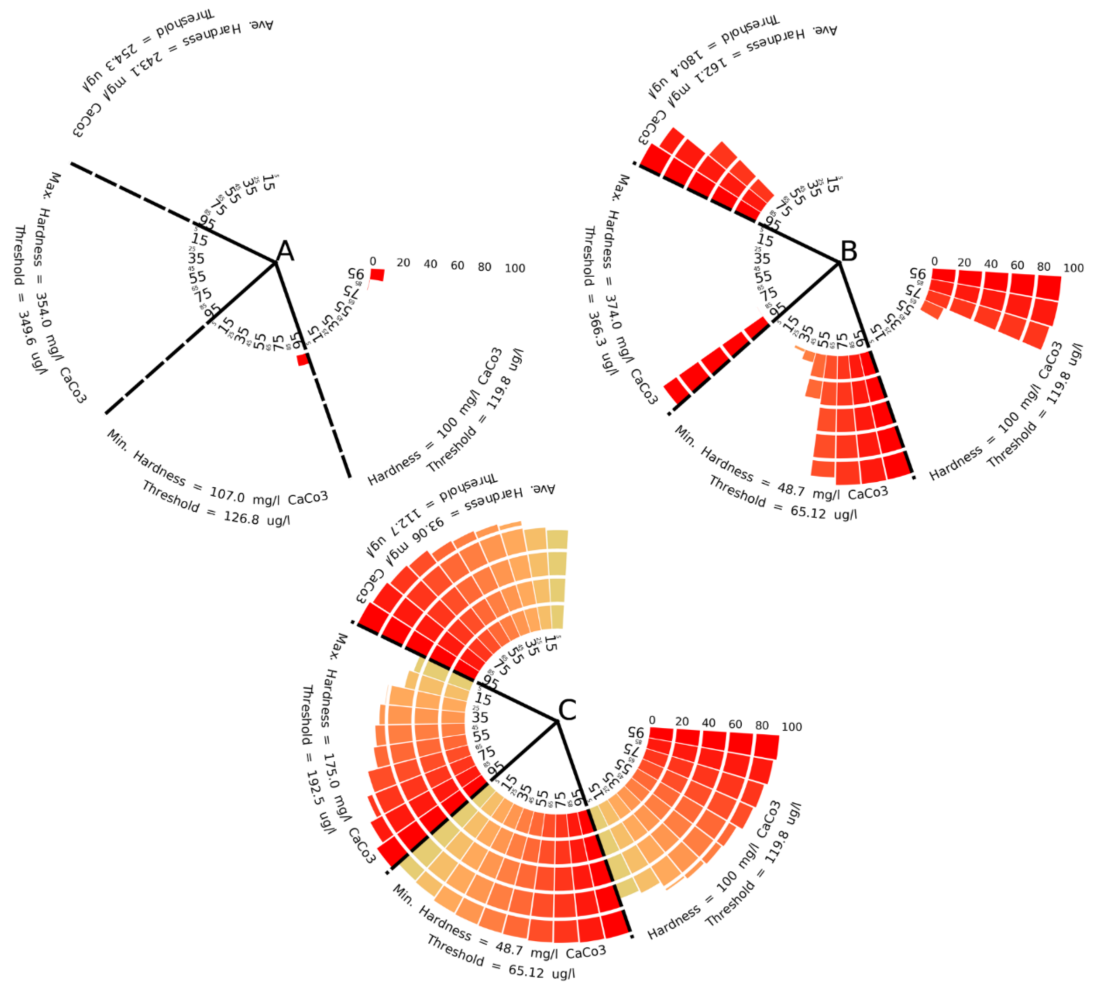


*Figure 6. Likelihood of hazard posed by zinc concentration exceeding EPA maximum allowable threshold under different suspended sediment concentrations in cold season (A), warm season (B), and stormflow condition (C). Each plot includes four scenarios: average, minimum, and maximum observed hardness, as well as a constant hardness level of 100 $/l\ CaCo_3$, and their associated maximum allowable pollutant level. Each bin in each scenario is associated with one SSC level (percentile), the length of which represents probability of hazard. Bins are color-coded from yellow (low SSC level) to red (high SSC level).*

This is an author-produced, peer-reviewed version of this article. The final, definitive version of this document can be found online at *Science of the Total Environment*, published by Elsevier. Copyright restrictions may apply. doi: 10.1016/j.scitotenv.2019.134875

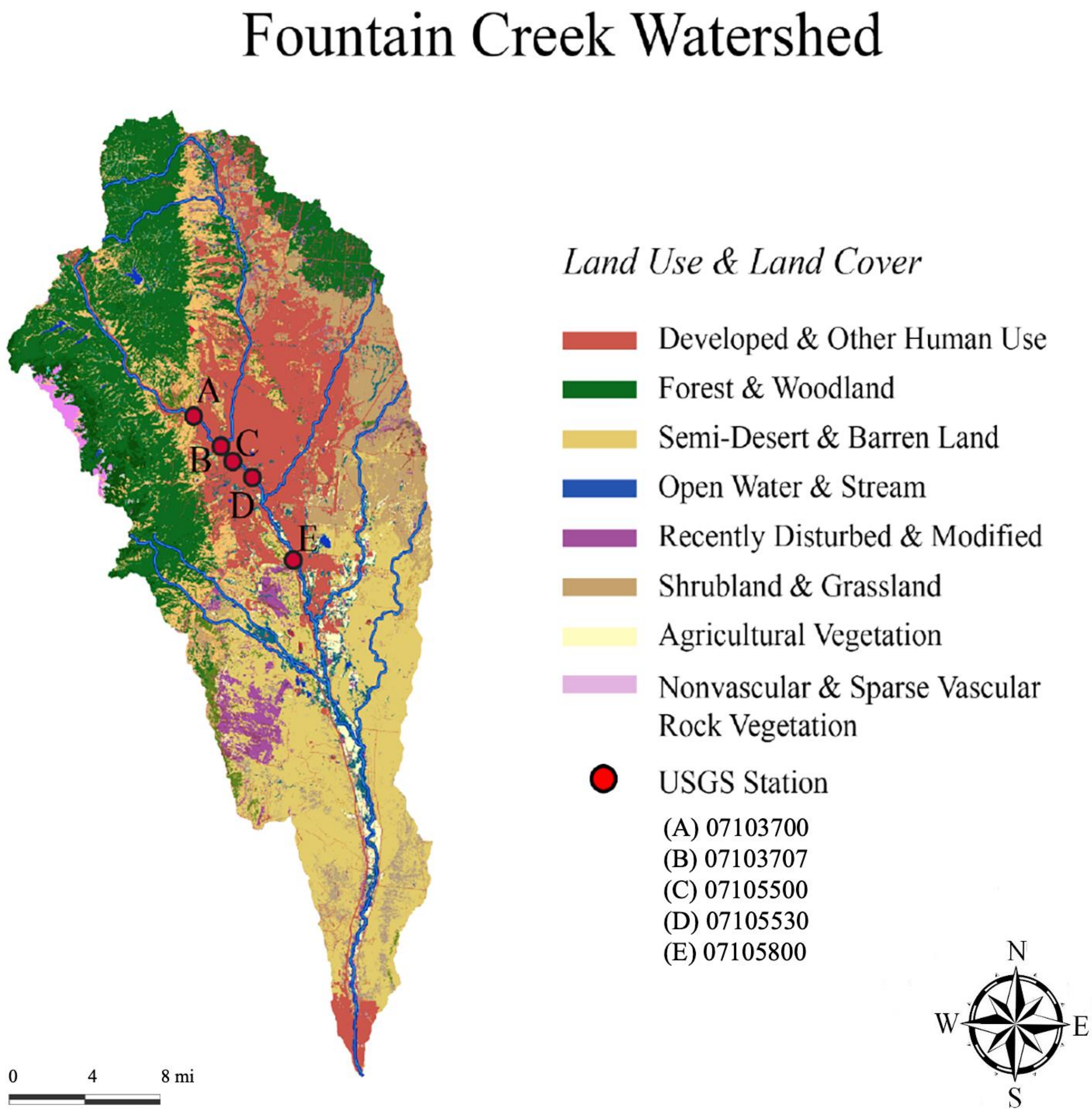


*Figure 7. Land use and land cover of the Fountain Creek watershed in Colorado monitored at several stations: (A) USGS-077103700, (B) USGS-07103707, (C) USGS-07105500, (D) USGS-07105530 and (E) USGS-07105800*

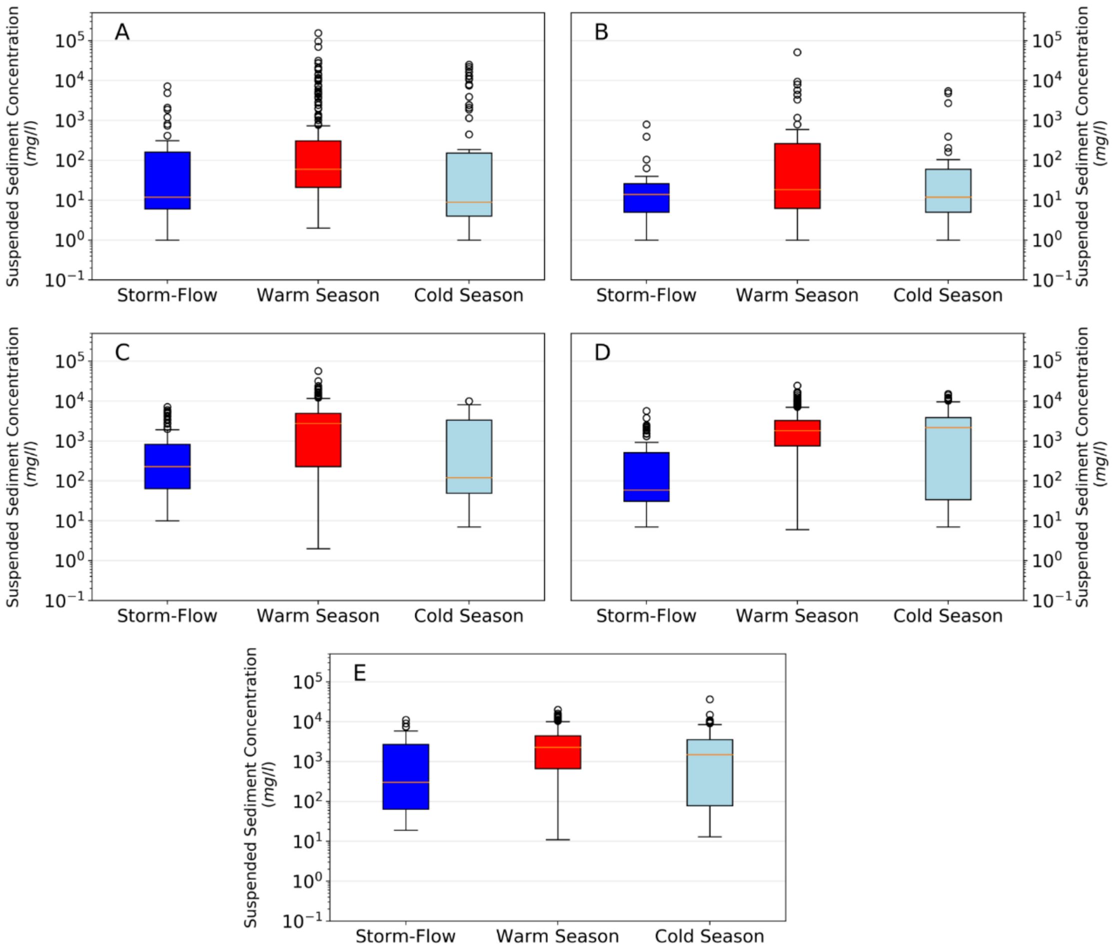


*Figure 8. Range of suspended sediment concentration under cold and warm seasons and stormflow condition for the monitoring stations on Fountain Creek: (A) USGS-077103700, (B) USGS-07103707, (C) USGS-07105500, (D) USGS-07105530 and (E) USGS-07105800*

This is an author-produced, peer-reviewed version of this article. The final, definitive version of this document can be found online at *Science of the Total Environment*, published by Elsevier. Copyright restrictions may apply. doi: 10.1016/j.scitotenv.2019.134875

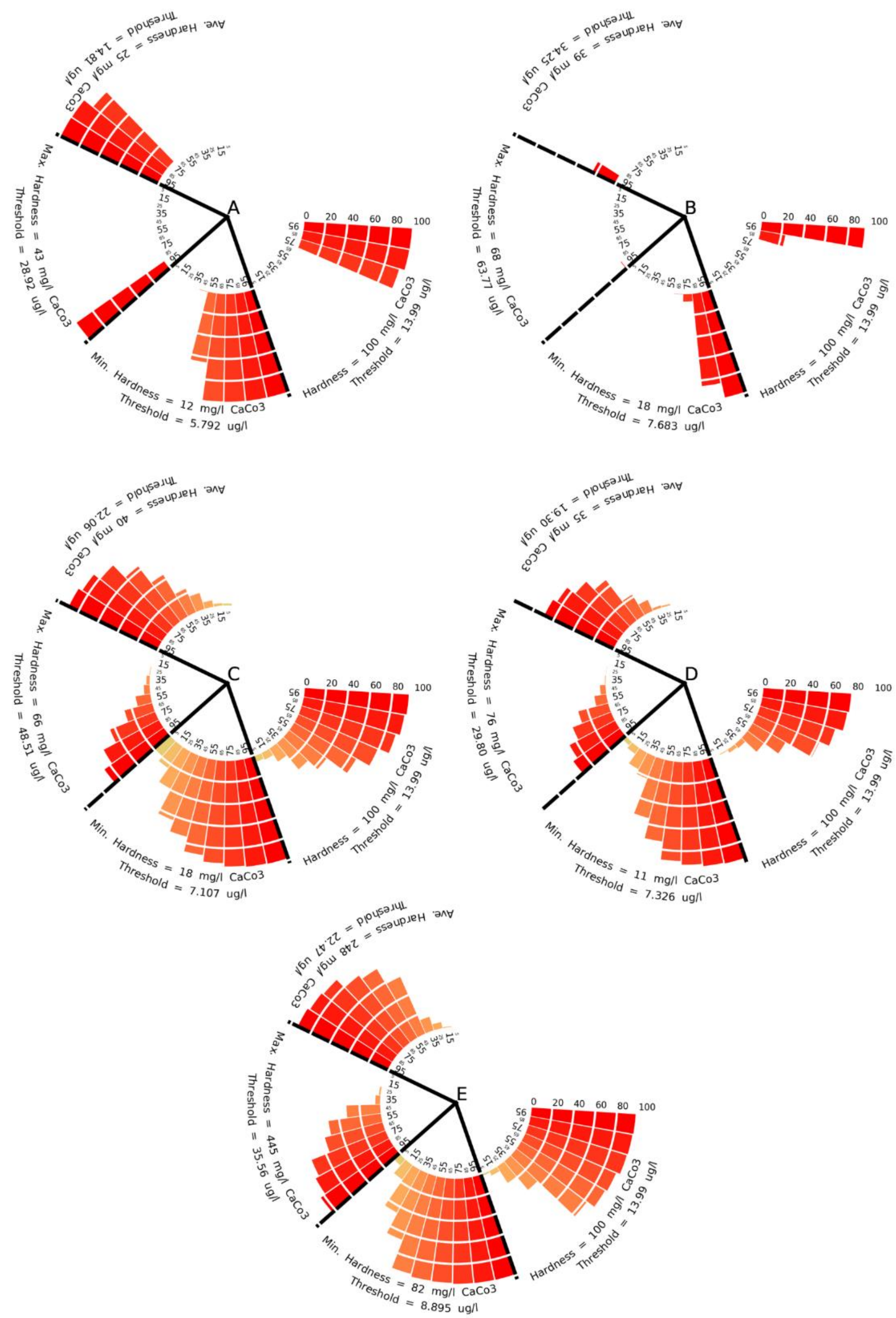


*Figure 9. Likelihood of hazard posed by copper concentration exceeding EPA maximum allowable threshold under warm season for different stations on Fountain Creek: (A) USGS-077103700, (B) USGS-07103707, (C) USGS-07105500, (D) USGS-07105530 and (D) USGS-07105800. Each plot includes four scenarios: average, minimum, and maximum observed hardness, as well as a constant hardness level of 100 $mg/l\ CaCo_3$ , and their associated maximum allowable pollutant level. Each bin in each scenario is associated with one SSC level (percentile), the length of which represents probability of hazard. Bins are color-coded from yellow (low SSC level) to red (high SSC level).*